



**HAL**  
open science

## Numerical Characterization of Acoustic Properties of A Novel Bio-based Porous Epoxy Resin

Quoc Bao Nguyen, Vu-Hieu Nguyen, Agustun Rios De Anda, Davy-Louis Versace, Estelle Renard, Salah Naili

► **To cite this version:**

Quoc Bao Nguyen, Vu-Hieu Nguyen, Agustun Rios De Anda, Davy-Louis Versace, Estelle Renard, et al.. Numerical Characterization of Acoustic Properties of A Novel Bio-based Porous Epoxy Resin. Forum Acusticum, Dec 2020, Lyon, France. pp.1847-1854, 10.48465/fa.2020.1007 . hal-03240359

**HAL Id: hal-03240359**

**<https://hal.science/hal-03240359>**

Submitted on 30 May 2021

**HAL** is a multi-disciplinary open access archive for the deposit and dissemination of scientific research documents, whether they are published or not. The documents may come from teaching and research institutions in France or abroad, or from public or private research centers.

L'archive ouverte pluridisciplinaire **HAL**, est destinée au dépôt et à la diffusion de documents scientifiques de niveau recherche, publiés ou non, émanant des établissements d'enseignement et de recherche français ou étrangers, des laboratoires publics ou privés.

# NUMERICAL CHARACTERIZATION OF ACOUSTIC PROPERTIES OF A NOVEL BIO-BASED POROUS EPOXY RESIN

Q.-B. Nguyen<sup>1,2,3</sup>

V.-H. Nguyen<sup>1,2</sup>

C. Perrot<sup>4</sup>

A. Rios de Anda<sup>3</sup>

E. Renard<sup>3</sup>

S. Naili<sup>1,2,\*</sup>

<sup>1</sup> Univ Paris Est Creteil, CNRS, MSME, F-94010 Creteil, France

<sup>2</sup> Univ Gustave Eiffel, MSME, F-77447 Marne-la-Vallée, France

<sup>3</sup> Univ Paris Est Creteil, CNRS, ICMPE, F-94010 Creteil, France

<sup>4</sup> MSME, Univ Gustave Eiffel, UPEC, CNRS, F-77454, Marne-la-Vallée, France

naili@u-pec.fr

## ABSTRACT

This work aims at studying acoustic properties of a novel bio-based porous epoxy resin obtained by an adapted combination of cationic photopolymerization and porogen leaching technique. A multiscale framework was applied to characterize numerically the sound absorption performances of a plate-like panel made of this kind of material. Within this framework, the asymptotic homogenization method was first used to estimate the effective properties of the elaborated material, which has fillet-edge cubic pore shapes according to the SEM (Scanning electron microscope) images. The finite element method was used to solve the cell problems and compute the effective properties. The sound absorption of a plate made by the equivalent poroelastic material with rigid impervious backing under a normal incidence was then studied. The validation was done by comparing the numerical estimation of equivalent dynamic density and bulk modulus to corresponding experimental results obtained by using the three-microphone impedance tube testing on several elaborated samples. A parametric study was then carried out to investigate influences of the porosity, the pore arrangement, and the pore size on sound absorption performances of the material. The obtained results should be very useful for improving the elaboration process of the material in order to optimize, in particular, the sound absorption performances of isolation structures.

## 1. INTRODUCTION

Porous materials are widely used in acoustic applications such as protection and isolation. However, most of them are petro-based polymers obtained by using solvents and toxic amine-type hardeners, raising environment and health problems. In order to tackle this concern, a novel bio-based porous epoxy resin resulting from an adapted combination of the cationic photopolymerization of a resorcinol derivative extracted from biomasses [1] and the porogen leaching technique [2] has been developed.

To characterize acoustic properties of porous materials, one can carry out experimental methods such as impedance tube testing involved in transfer functions. Nonetheless,

conducting acoustic experiments normally needs specific facilities and enormous effort, especially when parametric studies are expected. Additionally, the measurement methods in the acoustic domain are not always capable of capturing relations between microstructures and properties of materials. Therefore, the application of modeling tools to characterize numerically acoustic behaviour of porous materials becomes a crucial demand, especially for the stage in which materials are being developed.

Among the methods of modeling porous materials, the asymptotic homogenization is one of the most convenient and commonly accepted methods which allow to estimate all effective properties of a poroelastic medium. This method has been used with success in several recent papers to characterize new materials [3, 4]. Based on the effective properties obtained by the asymptotic homogenization, one can deal with sound absorption problems related to the studied porous material with boundary conditions of interest. The fact that the homogenization theory starts at the microscopic scale with the linearized equations of elasticity and the linearized equations of fluid dynamics, accompanied by the availability of a detailed microstructure of the pores with the assumption of periodicity (see for instance [5] for a mechanical point of view and [6] for a mathematical point of view), enables to establish relations between microstructural parameters and sound absorption performance of the material.

It is well-known that the material properties of the solid phase, the pore size, the porosity and the pore arrangement have substantial impacts on the acoustic performance of porous materials. Research works in the literature have mainly concentrated on the idealized microstructures with spherical, cylindrical, cross-type or sometimes polyhedral pores [7, 8]. To the best of our knowledge, there is a shortage of studies of the influence of microstructural parameters related to the case of interconnected fillet-edge cubic pores which imitate the pores of the aforementioned novel porous bio-based epoxy resin and generate more complex morphology than the ones previously cited.

The main objective of this study is to perform numerical characterization of acoustic properties of the novel bio-inspired porous epoxy resin, which is produced by combin-

ing adequately the cationic photopolymerization and the porogen leaching technique. The paper provides original insights into the influences of the microstructural characteristics, namely the pore arrangement, the porosity, and finally, the pore size on the acoustic behaviour of the porous material possessing interconnected pores with the specific fillet-edge cubic shape. To the authors' knowledge, the features of this microstructure resulting from the application of the porogen leaching technique have been considered merely in a very limited number of studies in the literature. The obtained results may allow us to make essential suggestions for improving the acoustic performance of the material of interest.

For numerically characterizing the elaborated porous material, a multiscale approach based on the asymptotic homogenization has been employed. The resolution of cell problems derived by this method has been conducted by considering idealized cell structures obtained from experimental pore characterizations of sample microstructures. Using homogenization results, the normal incidence sound absorption problem of a porous plate made of the studied material has been studied. The mechanical model has been validated by a comparison between the numerical results of acoustic properties, namely equivalent dynamic density and bulk modulus, and the corresponding measurements obtained by the three-microphone impedance tube testing. The multiscale approach has been then applied to investigate the effects of microstructural features on the acoustic behaviour of the material. For this purpose, four different ordered pore arrangements as well as systematic variations of the porosity and the pore size have been taken into account.

## 2. MATERIAL ELABORATION AND EXPERIMENTAL PORE CHARACTERIZATION

The porous epoxy resin synthesized from resorcinol diglycidyl ether was elaborated by means of the cationic photopolymerization in conjunction with the porogen leaching technique which involved the use of chloride sodium (NaCl) particles as solid porogens. The key idea of introducing NaCl particles in the formulation is that the removal of these salt particles by water after cross-linking will leave the empty space, generating porosity in the obtained material. Cylindrical NaCl templates with a diameter of 5.1 cm and a height of 0.5 cm were fabricated by the Spark Plasma Sintering (SPS) technique using 250-400  $\mu\text{m}$  NaCl particles. This sintering technique consists in simultaneous variations of heat and pressure on NaCl particles, creating the contacts among these particles and hence enabling the pore interconnection of the obtained porous material [9]. Based on NaCl mass and the dimensions of the templates, salt volume fraction is about 82%.

Pore features of the obtained porous material was then characterized by Mercury Intrusion Porosimetry (MIP) and Scanning Electron Microscopy (SEM). According to MIP results, the distribution of pore size is centered at about 180  $\mu\text{m}$ . This value is smaller than the size of NaCl particles used in the fabrication of templates (*i.e.*, 250-400  $\mu\text{m}$ )

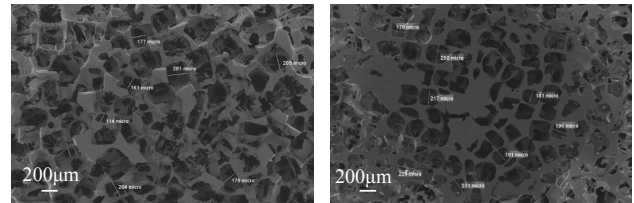


**Figure 1.** SEM micrographs: (left) on cross-section; (right) on external surface

due to the fact that during the tests by MIP, at each level of mercury pressure, one measures the largest entrance towards a pore, but not the actual inner size of a pore [10]. The dimension of this entrance is smaller than the inner pore size which is similar to the particle size. The analysis of SEM micrographs (see Fig. 1) gives the average value of entrance dimension which is about 192  $\mu\text{m}$ , showing a good agreement with the profile obtained by the MIP. The porosity of the synthetic porous material was identified by gravimetric and geometric methods, giving the value of approximately 83% which correlates with the NaCl volume fraction of 82%.

## 3. MULTISCALE APPROACH

In this work, a two-scale asymptotic homogenization procedure is applied and its details can be found in many studies such as [11, 12]. Within this procedure, physical variables are expanded asymptotically in terms of functions which are periodic with the period of a unit cell and a scale ratio which is the ratio of the unit length of periodicity and the macroscopic characteristic length. The introduction of these asymptotic expansions to linearized equations of elasticity, of fluid dynamics and of the thermal field followed by consideration of terms corresponding to specific orders of the scale ratio leads to cell problems. The resolution of these cell problems performed by using the finite element method on the unit cell with periodic conditions allows to obtain characteristic functions which are used to compute effective properties of the porous material such as effective elasticity tensor, effective dynamic density tensor and effective dynamic bulk modulus. The equivalent dynamic density and bulk modulus can be expressed in terms of effective dynamic density and bulk modulus as described in [13] and [14], respectively. The homogenization procedure also enables the derivation of macroscopic constitutive equations and macroscopic governing equations of the homogenized medium.

Based on the homogenization results, a normal incidence sound absorption problem is then considered for a plate of a given thickness which is made of the studied material with a rigid impervious backing at one side and surrounded by the air from another. Such a problem is described in detail in [15, 16] concerning the determination of the surface impedance at the front surface of the plate and then the calculations of the sound reflection and absorption coefficients from the computed surface impedance.

#### 4. CONSTRUCTION OF IDEALIZED ELEMENTARY PORE AND MATRIX

The construction of a unit cell was based on three factors: pore shape, pore entrance dimension and porosity. In the context of the NaCl leaching technique, the pore shape is associated strictly with the shape of NaCl particles. The fact that NaCl crystals used in this work have the cubic shape as confirmed by the SEM image of NaCl particles in Fig. 2a allows to consider the shape of resulting pores as cubic, more precisely cubic pores with fillet external edges (see Fig. 2c).

Because the mode “face to face” of the fusion of NaCl cubic particles has been more frequently found in SEM micrographs (see Figs. 1 and 2b), this mode was chosen to construct the unit cell, leading to square-shaped pore entrances. From the MIP profile, these square entrances were considered to have the side dimension  $l_t = 180 \mu\text{m}$  (see Fig. 2d). To make the fillet-edge cubic pore for a porosity of 83% as mentioned above, an elementary cube with a side length  $l = 305 \mu\text{m}$  and three orthogonal cylinders with a radius of  $177 \mu\text{m}$  and a length of  $305 \mu\text{m}$  were created with the same center point. The elementary pore was then the intersection of the elementary cube and the three cylinders. Subsequently, the elementary matrix was the difference between the elementary cube and the elementary pore, (see Fig. 2d). The term “pore size” is hereafter used to refer to the side length of the elementary cube.

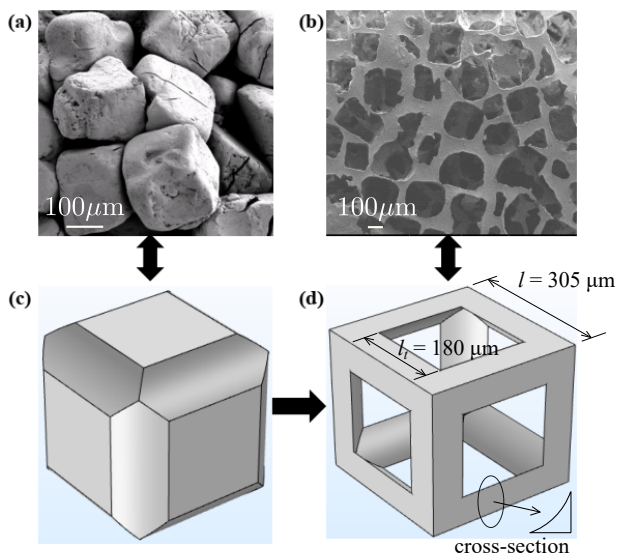


**Figure 2.** Construction of the elementary pore and matrix by the idealized periodic microstructure. (a) SEM image of sintered NaCl particles; (b) SEM image of the present porous material; (c) Elementary cubic pore; (d) Elementary cubic matrix.

#### 5. NUMERICAL RESULTS AND DISCUSSION

##### 5.1 Experimental validation

The cell problems are solved numerically with the use of a unit cell formed by the elementary cubic matrix (for

the solid phase - Fig. 2d) and the elementary cubic pore (for the fluid phase - Fig. 2c). In the study, it is assumed that each external plane surface of the unit cell is orthogonal to a basis vector of the Cartesian coordinate system. Note that this unit cells are cubic symmetric and this characteristic ensures its periodicity in three directions. The epoxy matrix is isotropic and its elasticity tensor is characterized by two independent coefficients, Young’s modulus  $E^s = 4.5 \times 10^9 \text{ Pa}$  and Poisson’s ratio  $\nu^s = 0.34$ . Its density is given by  $\rho^s = 1318 \text{ kg/m}^3$ . The fluid phase is taken to be the air with following properties: density  $\rho^f = 1.225 \text{ kg/m}^3$ , dynamic viscosity  $\eta = 1.81 \times 10^{-5} \text{ Pa.s}$ , characteristic thermal conductivity  $\kappa_0^f = 2.41 \times 10^{-2} \text{ W/(m.K)}$ , specific heat ratio  $\gamma^f = 1.4$  at the pressure at rest  $P^f = 101325 \text{ Pa}$ . The sound velocity in the air is given as  $c_0 = 331.6 \text{ m/s}$ .

The experimental validation of the model is performed by implementing three-microphone impedance tube experiments on the porous material for which the acoustic properties including equivalent dynamic density and bulk modulus are measured. The configuration of the experiments is shown in Fig. 3. Two samples having the cylindrical shapes with a thickness of 0.5 cm and a diameter of 4 cm were tested. For each sample, two experiments were conducted for two opposite incidence surfaces. The experiments were carried out for the range of frequencies from 4 to 4500 Hz, in condition of rigid impervious backing and normal incidence with acoustic plane waves.

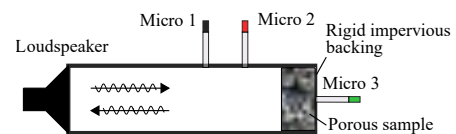


**Figure 3.** Configuration of three-microphone impedance tube experiments.

The numerical and experimental results of the equivalent dynamic density and bulk modulus are plotted in Fig. 4. In this figure, the experimental results are presented in terms of mean values along with corresponding error bars at each frequency. The green and cyan colours are used for the standard deviation. A good agreement between modeling results and corresponding measurements is figured out for these two parameters in the frequency range beyond 1000 Hz. For lower frequencies, there exist fluctuations in the experimental values of both parameters and accordingly the deviations of modeling results from experimental ones. These divergences may be attributed to the lack of accuracy due to edge constraints on small samples. In addition, the mismatch occurring below 1000 Hz may be explained by the dependence of the three-microphone impedance tube testing on the upstream microphones inter-spacing which becomes too small compared to large wavelengths and lowers the accuracy of the testing method [17]. Despite a little mismatch below 1000 Hz, the above numerical results are considered as satisfying enough so that the multiscale approach can be applied in the next step to investigate the influences of mi-

crostructural features, namely pore arrangements, porosity and pore size, on the acoustic behaviour of the material.

## 5.2 Effect of pore arrangements on sound absorption

Based on the obtained elementary cubic pore and elementary matrix presented in section 4, the unit cells corresponding to four different ordered arrangements of pores are established (Fig. 5). It is noted that the unit cell used in section 5.1 implies the consideration of arrangement 1. This choice allows to simplify the geometry of the unit cell and to validate the model with ease. In this section, for deeper understandings of effects of pore arrangements on the effective properties and the sound absorption performance of the material, other arrangements with more complex unit cells are taken into account. Because the use of the elementary cube as a unit cell is enough to express arrangement 1 and the symmetry of the cube ensures the periodicity in three directions, the unit cell in this case has the side length of  $l$ . For the other arrangements, the corresponding unit cells are cubic volumes with side length of  $2l$  and are constructed in a manner so that each arrangement is well represented and the periodic conditions are satisfied. All considered unit cells possess the orthotropic symmetry in which there are 3 mutually orthogonal planes of reflection symmetry; especially, the unit cell for arrangement 1 refers to the cubic symmetry with also  $90^\circ$  rotation symmetry with respect to those planes while the unit cells for arrangements 3 and 4 involve the transversely isotropy with additional axial symmetry about an axis (in Fig. 5, it is the axis orthogonal to the square-marked surface for arrangement 3 and to the star-marked surface for arrangement 4). It is also worth noting that all of unit cells have the porosity of 83%, meaning that the porosity in case of cubic pores is independent on pore arrangements.

The dependence of sound absorption on pore arrangements is illustrated in Fig. 6. In this figure, the sound absorption coefficient has been calculated for different incidence directions which are orthogonal to the star-, square- and circle-marked surfaces defined in Fig. 5. From Figs. 6, it is noted that the symmetry characteristics for different pore arrangements are well represented. Arrangement 1 with cubic symmetry gives the material with the same sound absorption coefficient for all three directions. Two arrangements with transverse isotropy result in materials of which sound absorption coefficient is the same for 2 directions orthogonal to the axis of rotation symmetry.

Regarding arrangement 1, a remark is made for the low sound absorption coefficient in this case compared to those in other arrangements. This result is related to the fact that the microstructure of the material resulting from arrangement 1 has a larger pore entrance dimension compared to those for other configurations. This leads to the decrease of viscous damping and thermal dissipation, and therefore, results in less effective sound absorption. This phenomenon is also observed in some parametric studies carried out in two dimensions for fibrous media [18] as well as in three dimensions for foams [8]. Because the pore arrangement duplicates the arrangement of porogen parti-

cles, we can link the porogen arrangement and the sound absorption. Although the porogen arrangement is not controlled yet in the present elaboration process, the results of this section suggest that the arrangement of porogen particles should fall into types 2, 3 or 4 for the possibly highest sound absorption.

## 5.3 Effect of porosity on sound absorption

Three cases of porosity, namely 69%, 83% and 96%, are under consideration in the context of arrangement 1 in order to investigate the influence of porosity on acoustic behaviour of the material. The porosity is varied in a manner so that the pore size which is also the unit cell size remains unchanged and has the value  $l = 305 \mu\text{m}$ .

The effect of porosity on the sound absorption coefficient of the material is highlighted by Fig. 7. While the absorption coefficient increases slightly according to the rise of the porosity within the range of frequencies below 1000 Hz, a noticeable improvement on the sound absorption is observed with the decrease in the porosity for higher frequencies. These results suggest that for a better sound absorption at frequencies lower than 1000 Hz, there needs more porosity, which can be achieved by raising the pressure and the temperature during the SPS process to have more porogen constituents in a volume. On the contrary, within the range of higher frequencies, a reduction in porosity is expected to favour the sound absorption performance of the porous material, which can be made available by a decrease in SPS pressure and temperature. Nevertheless, pressure and temperature should not be too low in order to allow porogen fusion and ensure the pore interconnection. This implies the existence of optimal values of pressure and temperature during the SPS process for attainment of materials with interconnected pore networks exhibiting the best sound absorption performance at higher frequencies.

## 5.4 Effect of pore size on sound absorption

The relation between the pore size and the acoustic behaviour of the resulting material are studied through simulations in which arrangement 1 is taken into account and the pore size is varied while keeping the porosity at 83%. Because the pores are obtained by the NaCl removal, so the pore size can be considered ideally equal to the NaCl particle size. A variation of the pore size from 45 to 710  $\mu\text{m}$  with a step of 5  $\mu\text{m}$  is taken into account, based on the sieve sizes available on the market for sieving NaCl particles. To assess the sound absorption capacity of the material at low frequencies, a single number rating, namely normal incidence sound absorption average SAA, is calculated for each case of the pore size. This parameter is defined in the standard ASTM C423 [20] as the average, rounded off to the nearest 0.01, of the sound absorption coefficients of a material for the twelve one-third octave bands from 200 through 2500 Hz inclusive, namely 200, 250, 315, 400, 500, 630, 800, 1000, 1250, 1600, 2000 and 2500 Hz. The SAA varies from 0 to 1: SAA = 0 indicates a perfect sound reflection, whereas SAA = 1 indicates a

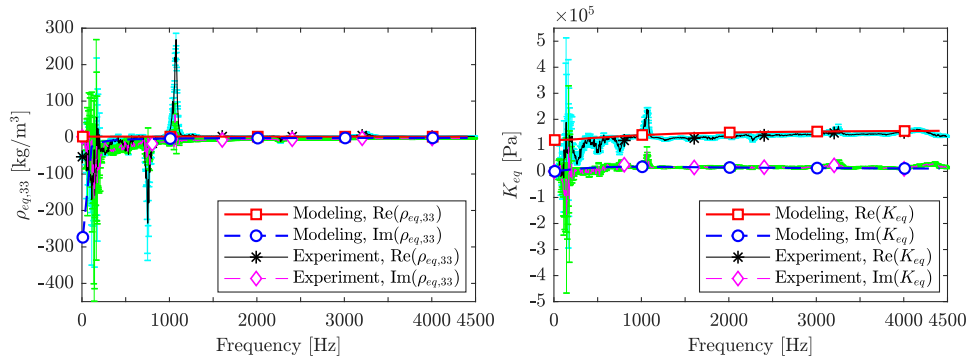


**Figure 4.** Comparison of numerical and experimental results of equivalent dynamic density component  $\rho_{eq,33}$  (left) and equivalent dynamic bulk modulus  $K_{eq}$  (right). The sample thickness is 0.5 cm. The green and cyan colours are used for the standard deviation.

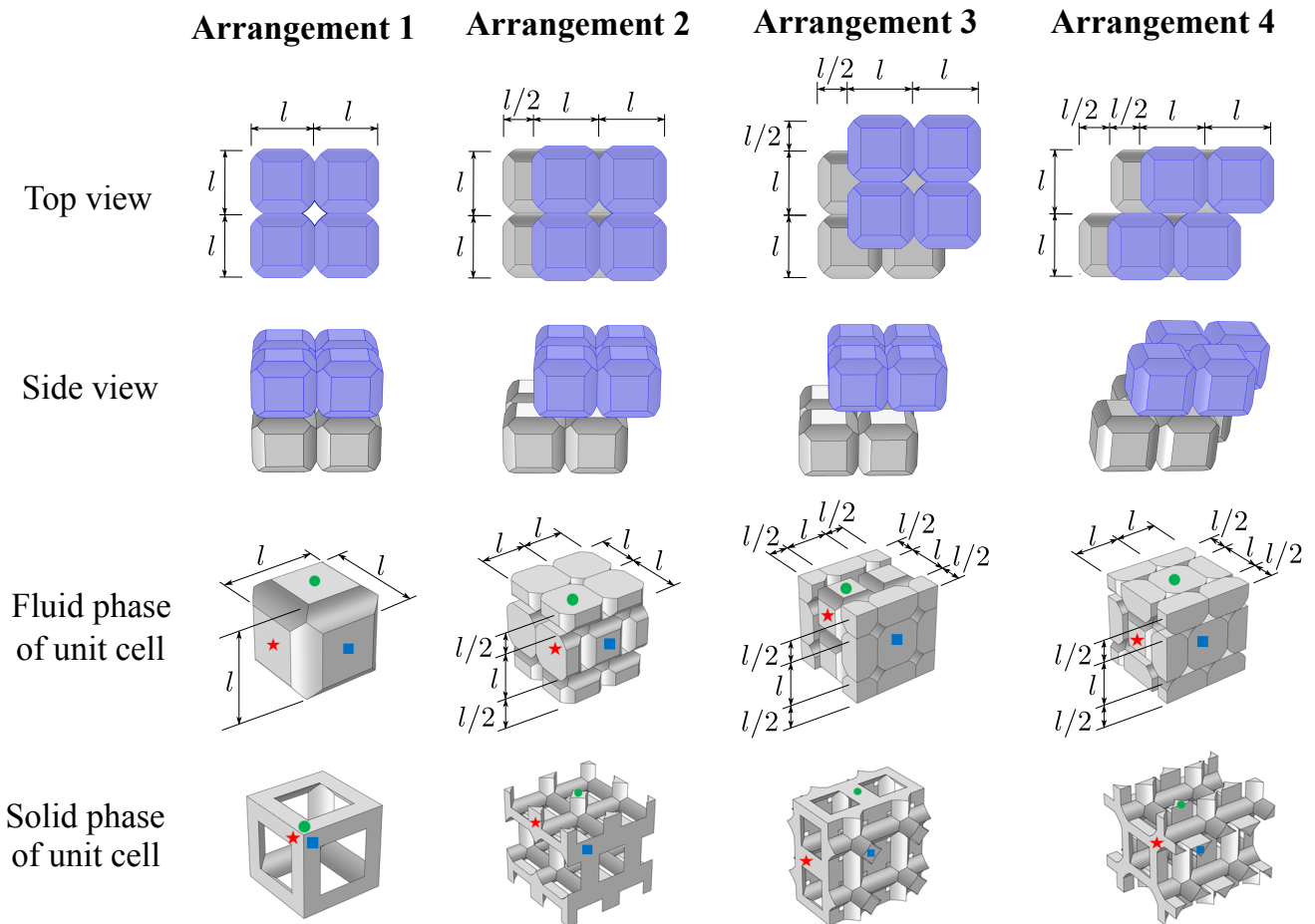


**Figure 5.** Unit cells of different pore arrangements. The star-, square- and circle-marked surfaces correspond to the surface orthogonal to the normal sound incidence direction.

perfect sound absorption [21]. The results of these simulations are presented in Fig. 8 where the evolution of the SAA for different cases of the pore size together with the porous plate's thickness is illustrated.

When the plate thickness is 0.5 cm, the SAA is relatively low with the maximum value of 0.12 at the pore size of  $45 \mu\text{m}$ . For this plate, the increase in the pore size from  $45$  to  $710 \mu\text{m}$  provokes the decrease in the SAA. This behaviour is explained by noting that the increase in the pore

size enlarges the cross-sectional area of the fluid phase, weakening the viscosity effect as well as the thermal dissipation and thus reducing the sound absorption capability [12].

When the plate becomes thicker, *i.e.* 2, 10 and 20 cm thickness, the SAA is considerably enhanced. This improvement in sound absorption performance is attributed to the increase in the plate thickness which means more restriction on the propagation of sound waves from the front

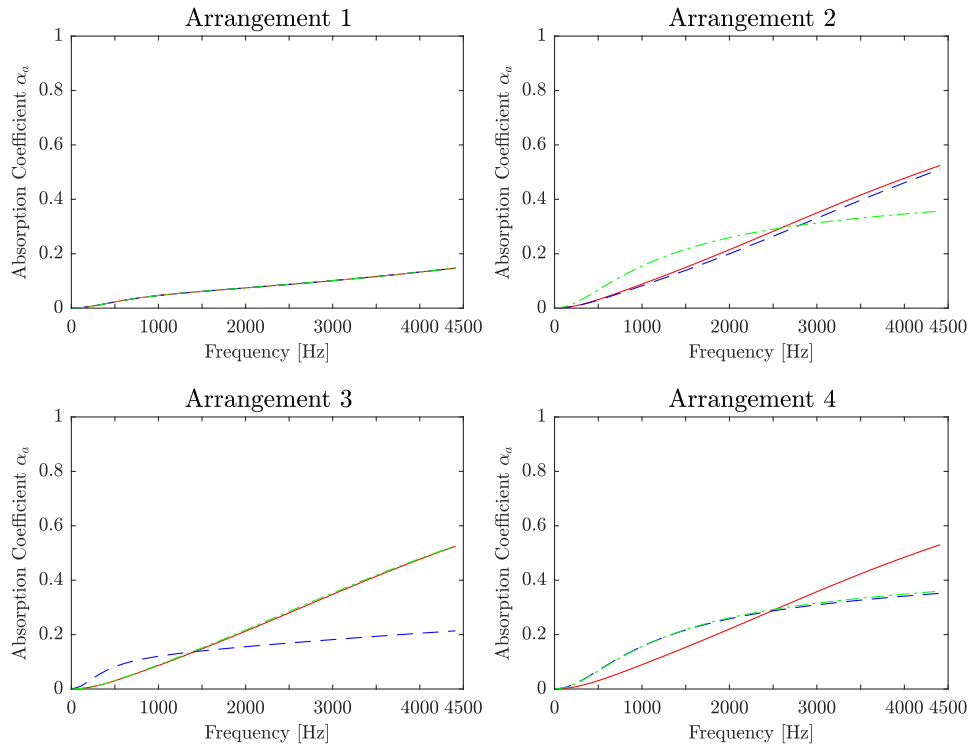


**Figure 6.** Dependence of sound absorption coefficients on different pore arrangements. The plate thickness is 0.5 cm. Solid, dashed and dashed-dot lines correspond to cases in which star-, square- and circle-marked surfaces of unit cells are orthogonal to the normal incidence direction, respectively.

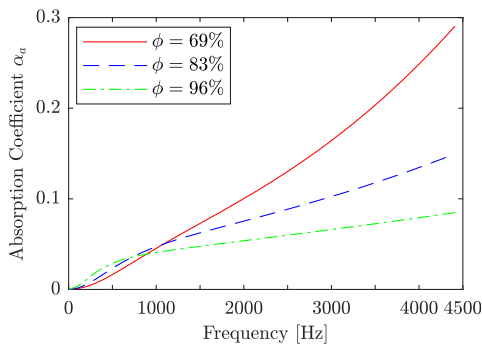


**Figure 7.** Dependence of sound absorption coefficient on porosity. The plate thickness is 0.5 cm.

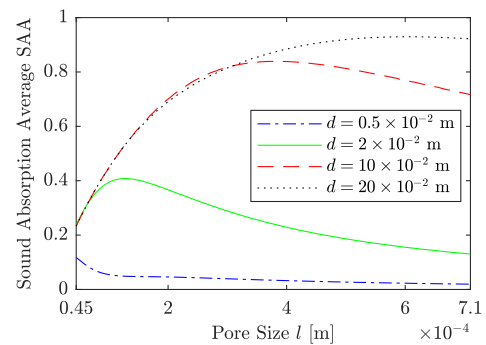


**Figure 8.** Normal incidence sound absorption average SAA for different cases of the pore size and the porous plate's thickness. The porosity is fixed at  $\phi = 83\%$ .

to the back of the plate and hence more attenuated sound energy. Moreover, the attention is paid to the appearance of the peaks of the pore size *versus* SAA curves for these three cases of plate thickness. Generally, the increase of the pore size leads to the entrance of more sound waves. When the pores size is not too large for a given plate thickness and the viscous as well as thermal effects are still important to afford these entering sound waves (left-hand side of the peaks), increasing the pore size leads to more attenuated sound energy, meaning the improvement of the SAA. Conversely, when the pore size continues to increase (right-hand side of the peaks), the cross-sectional area of the fluid phase becomes too large, reducing viscous damping together with thermal dissipation and therefore result-

ing in less effective sound absorption. One can also observe similar peaks with two opposite trends in [22] for pores of cylindrical cross-section shape and in [8] with Kelvin's cell (tetrakaidecahedron) for high porosity foams. Furthermore, Fig. 8 shows that the peak of the curve has a tendency to occur at the higher pore size according to the increase in the thickness of the plate. This trend of peak movement depicting the correlation of the pore size and the plate thickness supplies an idea for the material design. Because the pore size in this work refers to the porogen size, for a given porogen size (or a given plate thickness), one can choose the appropriate plate thickness (or an appropriate porogen size) based on Fig. 8 to obtain the best

sound absorption performance.

## 6. CONCLUSION

The acoustic behaviour of the new bio-based porous epoxy resin obtained by the environmentally friendly combination of cationic photopolymerization and porogen leaching technique was numerically characterized within this work through a multiscale approach. This approach consisted in using the asymptotic homogenization method to obtain macroscopic equations with effective properties of the porous material from pore-scale equations, and based on these results, a normal incidence sound absorption problem of a structural plate made of the studied material was taken into account to study the acoustic performance of the material. The fact that homogenization calculations were performed on unit cells comprising idealized fillet-edge cubic elementary pore and matrix obtained from experimental pore characterizations of the elaborated porous epoxy resin allowed to disclose the microstructure-acoustic behaviour relation associated with this material.

After validated by a good match between numerical estimation of equivalent dynamic density and bulk modulus and corresponding experimental results obtained by the three-microphone impedance tube testing, the multiscale framework was used to study parametrically the effects of microstructural characteristics, namely pore arrangements, porosity and pore size, on the sound absorption performance of the materials. Based on these results, suggestions related to the material elaboration process were made to attain porous epoxy resins with good sound absorption. Firstly, if porogen particles could be packed through an orderly way to prepare the template, the arrangements 2, 3 and 4 would be recommended rather than the arrangement 1 to get better sound absorption. Secondly, the increase in porosity by raising the pressure and the temperature during the SPS process is necessary to improve the sound absorption at very low frequencies, whereas the inverse effect is predicted for higher frequencies. Finally, because the pore size in this study also refers to the porogen size, the obtained pore size *versus* SAA curves corresponding to various plate thicknesses provide a practical guide for material elaboration: for a given plate thickness (or a given porogen size), an appropriate porogen size (or an appropriate plate thickness) can be determined to obtain the best sound absorption performance.

## 7. ACKNOWLEDGEMENTS

This work has benefited from a French government grant managed by ANR within the frame of the national program of Investments for the Future ANR-11-LABX-022-01 (LabEx MMCD project).

## 8. REFERENCES

- [1] Q.-B. Nguyen, N.-H. Nguyen, A. Rios de Anda, V.-H. Nguyen, D.-L. Versace, V. Langlois, S. Naili, and E. Renard, "Photocurable bulk epoxy resins based on resorcinol derivative through cationic polymerization," *Journal of Applied Polymer Science*, p. e49051, 2020.
- [2] H.-B. Ly, B. Le Droumaguet, V. Monchiet, and D. Grande, "Designing and modeling doubly porous polymeric materials," *The European Physical Journal Special Topics*, vol. 224, pp. 1689–1706, July 2015.
- [3] R. Del Toro, A. Bacigalupo, and M. Paggi, "Characterization of wave propagation in periodic viscoelastic materials via asymptotic-variational homogenization," *International Journal of Solids and Structures*, vol. 172-173, pp. 110–146, 2019.
- [4] M. De Bellis, A. Bacigalupo, and G. Zavarise, "Characterization of hybrid piezoelectric nanogenerators through asymptotic homogenization," *Comput. Methods Appl. Mech. Engrg.*, vol. 355, p. 1148–1186, 2019.
- [5] J. L. Auriault, C. Boutin, and C. Geindreau, *Homogenization of Coupled Phenomena in Heterogenous Media*. Wiley-ISTE, 2009.
- [6] A. Mielke and E. Rohan, "Homogenization of elastic waves in fluid-saturated porous media using the biot model," *Mathematical Models and Methods in Applied Sciences*, vol. 23, no. 5, pp. 873–916, 2013.
- [7] L. Maheo, P. Viot, D. Bernard, A. Chirazi, G. Ceglia, V. Schmitt, and O. Mondain-Monval, "Elastic behavior of multi-scale, open-cell foams," *Composites Part B: Engineering*, vol. 44, no. 1, pp. 172–183, 2013.
- [8] F. Chevillotte and C. Perrot, "Effect of the three-dimensional microstructure on the sound absorption of foams: A parametric study," *The Journal of the Acoustical Society of America*, vol. 142, pp. 1130–1140, Aug. 2017.
- [9] A. Azarniya, A. Azarniya, M. Safavi, M. Ahmadipour, M. Seraji, S. Sovizi, M. Saqaei, R. Yamanoglu, M. Soltaninejad, H. Hosseini, S. Ramakrishna, A. Kawasaki, S. Adams, and M. Reddy, "Physico-mechanical properties of porous materials by Spark Plasma Sintering," *Critical Reviews in Solid State and Materials Sciences*, pp. 1–44, Feb. 2019.
- [10] H. Giesche, "Mercury porosimetry: A general (practical) overview," *Particle & Particle Systems Characterization*, vol. 23, no. 1, pp. 9–19, 2006.
- [11] E. Rohan, S. Naili, R. Cimrman, and T. Lemaire, "Multiscale modeling of a fluid saturated medium with double porosity: Relevance to the compact bone," *Journal of the Mechanics and Physics of Solids*, vol. 60, no. 5, pp. 857 – 881, 2012.
- [12] T. Yamamoto, S. Maruyama, K. Terada, K. Izui, and S. Nishiwaki, "A generalized macroscopic model for sound-absorbing poroelastic media using the homogenization method," *Computer Methods in Applied Mechanics and Engineering*, vol. 200, no. 1-4, pp. 251–264, 2011.

- [13] R. Panneton and X. Olny, “Acoustical determination of the parameters governing viscous dissipation in porous media,” *The Journal of the Acoustical Society of America*, vol. 119, no. 4, pp. 2027–2040, 2006.
- [14] X. Olny and R. Panneton, “Acoustical determination of the parameters governing thermal dissipation in porous media,” *The Journal of the Acoustical Society of America*, vol. 123, no. 2, pp. 814–824, 2008.
- [15] N. Gorbushin, V.-H. Nguyen, and S. Naili, “Design optimisation of acoustic absorbers with cross-like pores via a homogenisation method,” *Acta Acustica united with Acustica*, vol. 105, pp. 638–649, 2019.
- [16] N. Gorbushin, S. Naili, and V.-H. Nguyen, “Optimizing microstructure of a poroelastic layer with cylindrical pores for absorption properties,” *Mechanics Research Communications*, vol. 102, p. 103422, 2019.
- [17] Y. Salissou and R. Panneton, “Wideband characterization of the complex wave number and characteristic impedance of sound absorbers,” *The Journal of the Acoustical Society of America*, vol. 128, no. 5, pp. 2868–2876, 2010.
- [18] C. Perrot, F. Chevillotte, and R. Panneton, “Bottom-up approach for microstructure optimization of sound absorbing materials,” *The Journal of the Acoustical Society of America*, vol. 124, pp. 940–948, Aug. 2008.
- [19] L. Zhang, Y. Zhang, Y. Jiang, and R. Zhou, “Mechanical behaviors of porous Ti with high porosity and large pore size prepared by one-step spark plasma sintering technique,” *Vacuum*, vol. 122, pp. 187–194, Dec. 2015.
- [20] ASTM International, “Standard test method for sound absorption and sound absorption coefficients by the reverberation room method.” American Society for Testing and Materials, 2002.
- [21] M. Zainulabidin, M. Rani, N. Nezere, and A. Tobi, “Optimum sound absorption by materials fraction combination,” *International Journal of Mechanical & Mechatronics Engineering*, vol. 14, no. 02, p. 4, 2014.
- [22] G. Kirchhoff, “On the influence of heat conduction in a gas on sound propagation,” *R.B. Lindsay, Ed., Physical Acoustics*, pp. 7–19, 1974.